Production of Nonisothermal Electrons and Langmuir Waves Because of Colliding Ion Holes and Trapping of Plasmons in an Ion Hole

B. Eliasson and P. K. Shukla*

Institut für Theoretische Physik IV, Fakultät für Physik und Astronomie, Ruhr-Universität Bochum, D-44780 Bochum, Germany

(Received 25 September 2003; published 5 March 2004)

We present new simulation studies exhibiting production of nonisothermal electron distributions and Langmuir waves by colliding ion holes and trapping of plasmons in an ion hole. We find that, during head-on ion hole collisions, streams of accelerated electrons are produced by the electrostatic potentials supporting the ion holes. Subsequently, Langmuir waves are excited by a two-stream instability involving energetic electron beams. The resulting Langmuir waves can be trapped in an ion hole. The present ion-hole-Langmuir wave interactions are unique kinetic phenomena which can be dealt with a Vlasov code, which we developed recently. The results can have relevance to the understanding of particle and field data that are forthcoming from different spacecraft missions in Earth's auroral ionosphere and the magnetosphere.

DOI: 10.1103/PhysRevLett.92.095006 PACS numbers: 52.35.Mw, 52.35.Ra, 52.35.Sb, 94.30.Tz

Phase space electron and ion holes are typically associated with nonisothermal electron and ion distribution functions [1,2] that are far away from the Maxwellian distribution in plasmas. Phase space vortices are products of the two-stream instability in which linearly excited plasma modes acquire large amplitudes and saturate by trapping electrons or ions (depending on the phase speed of the waves) in the wave potential [3]. On the other hand, seed ion holes carrying plasmas can have a negative energy property, which implies that ion holes may grow even in linearly two-stream stable situations [4]. In the early seventies, Schamel [5] presented an elegant analytical method for finding physically acceptable solutions to the Vlasov-Poisson system. By prescribing both trapped and free particle distributions and by applying the so-called potential method, phase space holes [5,6] and double layer solutions [7] could be constructed which agree with laboratory observations [1]. Observations from laboratory experiments [8,9] and measurements from numerous spacecrafts [10–15] in Earth's auroral ionosphere and the magnetosphere reveal the formation of phase space electron and ion vortices and associated solitary waves/bipolar electric pulses. Computer simulation studies [16,17] also reveal the significance of phase space vortices in space plasmas. Magnetic field aligned large-scale electric fields and potentials are thought to be the main source of accelerated electrons found in Earth's auroral zone [10,11], where electrons are accelerated up to ten electron thermal speeds in the upward current region and to 10^4 electron thermal speeds in the downward current region.

In this Letter, we present for the first time new simulation results exhibiting collisions between two ion holes, which lead to the production of energetic electrons whose distribution function is nonisothermal on account of their acceleration by the localized (small-scale) electrostatic potentials of interacting ion holes. Streaming electrons, in turn, generate Langmuir waves via a two-stream instability. In the past, it has been shown that nonlinear interactions between Langmuir waves and nonresonant ion-acoustic perturbations give rise to new classes of envelope Langmuir solitons involving modified Boltzmann electron density distribution with [18] and without [19] trapped electron effects. Schamel and Maslov [20] presented an analytical description of Langmuir wave trapping in the density trough provided by the small amplitude electron hole. On the other hand, our simulation study here shows that Langmuir waves can be trapped in a large-amplitude ion hole, and that these Langmuir waves exhibit signatures of a downshifted frequency band compared to the surrounding plasma frequency, in agreement with our theoretical predictions [21]. We find that two counterpropagating finite amplitude ion holes are robust under head-on collisions. We note that the dynamics of elastically colliding small amplitude ion holes is governed by the modified Korteweg–de Vries equation [22], which admits some interesting integrability properties [23] based on Painlevé analysis and Baecklund transformation.

In order to investigate the time-dependent dynamics of the ion holes as well as kinetic effects for the electrons, we employ a newly developed code [24] which numerically solves the Vlasov-Poisson system of equations:

$$\frac{\partial f_j}{\partial t} + v\frac{\partial f_j}{\partial x} + \frac{q_j E}{m_j}\frac{\partial f_j}{\partial v} = 0, \tag{1}$$

$$-\frac{\partial^2 \phi}{\partial x^2} = 4\pi e \int_{-\infty}^{\infty} (f_i - f_e)\, dv, \qquad E = -\frac{\partial \phi}{\partial x}, \tag{2}$$

where f_j is the distribution function of the particle species j (j equals e for electrons and i for ions), m_j is the mass, $q_e = -e$, $q_i = e$, e is the magnitude of the electron charge, E is the electric field, and ϕ is the electrostatic potential. The initial conditions on f_i are set to the

Schamel distribution [1,6] for the free and trapped ions, which in the rest frame of the bulk plasma has the form

$$f_i = \begin{cases} n_0\left(\frac{m_i}{2\pi T_i}\right)^{1/2}\exp\left(-\frac{1}{2T_i}\{\pm[m_i(v-u_0)^2+2e\phi]^{1/2}+m_i^{1/2}u_0\}^2\right), & m_i(v-u_0)^2 > -2e\phi \\ n_0\left(\frac{m_i}{2\pi T_i}\right)^{1/2}\exp\left(-\frac{1}{2T_i}\{\alpha[m_i(v-u_0)^2+2e\phi]+m_iu_0^2\}\right), & m_i(v-u_0)^2 \le -2e\phi, \end{cases} \quad (3)$$

where u_0 is the speed of the ion hole and n_0 is the unperturbed ion (or electron) number density. Similar to an earlier investigation [21], we use $\alpha = -1.0$ and the electron to ion temperature ratio $T_e/T_i = 10$. The special choice of the initial condition (3) is motivated by the fact that it is also an exact solution of the ion Vlasov equation for the case when the potential $\phi = \phi(x - u_0 t)$, and it describes in this case a steady-state ion hole propagating with a constant speed u_0 [1,6]. The initial condition for the electron distribution function is taken to be the Maxwell-Boltzmann distribution,

$$f_e = n_0\left(\frac{m_e}{2\pi T_e}\right)^{1/2}\exp\left[\frac{1}{2T_e}(2e\phi - m_e v^2)\right]. \quad (4)$$

The potential ϕ for the initial conditions (3) and (4) is obtained by inserting them into Eq. (2), which is then integrated [6,21] to obtain the potential ϕ as a function of x; in practice, the integration of Eq. (2) is performed numerically. The potential thus obtained is then inserted into Eqs. (3) and (4) to obtain the ion and electron distribution functions.

The numerical solutions of the Vlasov-Poisson system were performed by means of a Fourier transform method [24]. We used 500 intervals in x space with the domain $-40 \le x/r_D \le 40$ with periodic boundary conditions, where $r_D = V_{T_e}/\omega_{p_e} = (T_e/4\pi n_0 e^2)^{1/2}$ is the electron Debye radius, $V_{T_e} = (T_e/m_e)^{1/2}$ is the electron thermal speed, and $\omega_{p_e} = (4\pi n_0 e^2/m_e)$ is the electron plasma frequency. We used 300 intervals in velocity space. The electron and ion speed intervals were in the ranges $-15.7 \le v/V_{T_e} \le 15.7$ and $-0.118 \le v/V_{T_e} \le 0.118$, respectively. The time step $\Delta t \approx 0.013\omega_{p_e}^{-1}$ was adapted dynamically to maintain numerical stability. We used $m_i/m_e = 1836$. First, we investigate the process of two colliding ion holes, as shown in Figs. 1–3. For the initial conditions, we considered that the ion holes initially are well separated in space, and that the interaction between the ion holes is weak, so that the solutions for the single ion holes can be matched in space to form an initial condition for the case with two ion holes. Figure 1 displays the features of the ion and electron distribution functions for two colliding ion holes, where initially (upper panels) the left ion hole propagates with the speed $u_0 = 0.9V_{T_i}$ and the right ion hole is standing. The ion and electron distribution functions associated with the ion holes are shown before collision at times $t = 0\omega_{p_i}^{-1}$ (upper panels) and $t = 35.9\omega_{p_i}^{-1}$ (middle panels), and after collision at time $t = 133\,\omega_{p_i}^{-1}$ (lower panels). Figure 1 exhibits that the ion holes undergo collisions without being destroyed; thus they are robust structures. As can be seen in the right panels of Fig. 1, the electrons have a strongly non-Maxwellian, flattop distribution in the region between the ion holes after collision has taken place. We have plotted the velocity distribution function against v/V_{T_e} in Fig. 2 at $x = 8.0r_D$. We see that the initial Maxwellian distribution (the upper panel) changes to a distribution with beams at $v \approx \pm 0.6V_{T_e}$ (the middle panel) slightly before collision, and to a flattop distribution with two maxima after collision (the lower panel). The reason for this phenomenon is that the two ion holes are associated with negative electrostatic potentials, and the electrons entering the region between the ion holes after collision must have a large enough kinetic energy to cross the potential barriers that are set up by the ion holes.

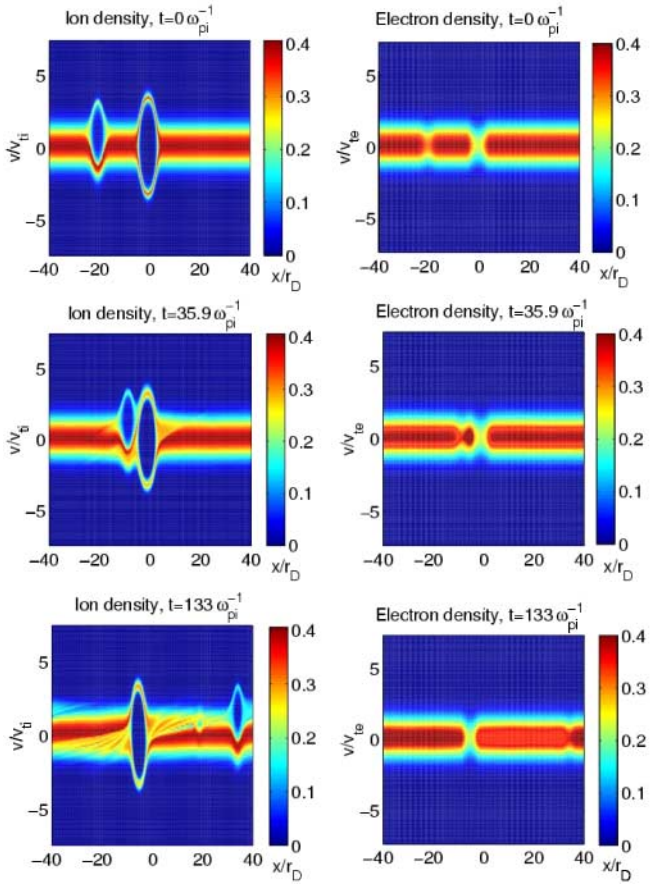

FIG. 1 (color online). The distribution function for the ions (left panels) and electrons (right panels) of two colliding ion holes, before the collision at times $t = 0\omega_{p_i}$ (upper panel) and $t = 35.9\omega_{p_i}$ (middle panel), and after the collision at $t = 133\omega_{p_i}$ (lower panel).

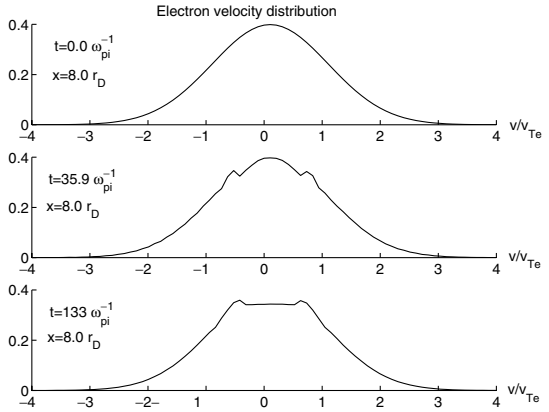

FIG. 2. The electron velocity distribution at $x = 8r_D$, for $t = 0\omega_{p_i}^{-1}$ (upper panel), $t = 35.9\omega_{p_i}^{-1}$ (middle panel), and $t = 133\omega_{p_i}^{-1}$ (lower panel).

Therefore, the region between the ion holes becomes excavated of low-energy electrons. On the other hand, we also observed that, before collision, the low-energy population of electrons was compressed between the ion holes (see the middle right panel of Fig. 1) and released during collision; these electrons were then accelerated to form the beams of electrons (see the middle panel of Fig. 2) which escape the ion holes. The energy of the electron beams was then released in a beam-plasma instability triggering Langmuir waves; see Fig. 3 (the left panel) where the electric field at $x = 8.0r_D$ is plotted as a function of $\omega_{p_i}t$. High-frequency Langmuir oscillations are beginning to be excited at time $t \approx 10\omega_{p_i}^{-1}$. The large-amplitude bipolar electric fields of the ion hole appear as it crosses $x = 8.0r_D$ at time $t \approx 50$–$80\omega_{p_i}^{-1}$. By examining the frequency spectrum of the electric field (the right panel), we notice that the Langmuir oscillations have frequency components which are slightly upshifted compared to the electron plasma frequency, and which can be attributed to waves with different wavelengths having frequencies higher than the plasma frequency according to the dispersion relation of Langmuir waves. We also have a slightly *downshifted* frequency band around $\omega/\omega_{p_e} = 0.9$, which we attribute to Langmuir waves trapped in an ion hole, as described below.

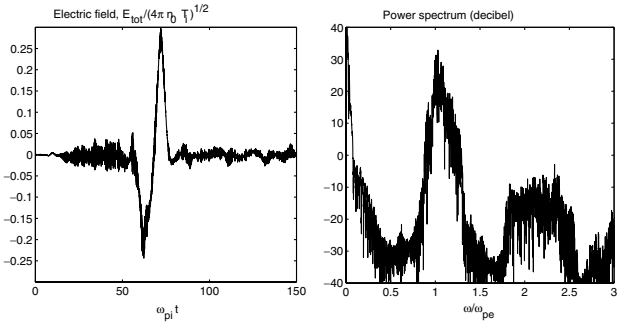

FIG. 3. The electric field at $x = 8.0r_D$ as a function of $\omega_{p_i}t$ (left panel) and the power spectrum of the electric field as a function of ω/ω_{p_e} (right panel).

In order to describe the trapping of Langmuir waves in an ion hole, we have performed a new set of simulations to study the time dependence of trapped Langmuir wave electric fields. The results are displayed in Fig. 4. In these simulations, the electron density is initially perturbed so that Langmuir waves are excited around the ion hole centered at $x/r_D = 0$. We examine an ion hole with zero speed (the left panel) and an ion hole having the speed $u_0 = 0.9V_{T_i}$ (the right panel). Figure 4 shows that Langmuir waves are trapped in the ion hole, with a maximum wave amplitude at $x/r_D = 0$. We find that the trapped Langmuir waves are oscillating with a real frequency slightly lower than the electron plasma frequency, $\omega_r/\omega_{p_e} \approx 0.93$ for the standing ion hole case and $\omega_r/\omega_{p_e} \approx 0.98$ for the moving ion hole case with $u_0 = 0.9V_{T_i}$. A previous theoretical investigation [21] revealed that the trapping of Langmuir waves in ion holes, with a Maxwell-Boltzmann distributed electrons, corresponding to the $\beta = 1$ case in Ref. [6] (a flattop distribution would correspond to the $\beta = 0$ case in Ref. [6]), can be described by a linear eigenvalue problem in the dimensionless form $3d^2W/d\xi^2 + [1 - \exp(\tau\phi) - \lambda]W = 0$ for the normalized (by $\sqrt{16\pi n_0 T_e}$) Langmuir wave electric field envelope W. Here λ is the eigenvalue, ϕ is the normalized (by T_i/e) electrostatic potential associated with the ion hole, ξ is the normalized (by the electron Debye radius) spatial variable, and $\tau = T_i/T_e$. Using the numerical values on the eigenvalue (the frequency shift) λ presented in Ref. [21], we obtain the theoretical values for ω which are displayed in Table I, and which follow the relation $\omega/\omega_{p_e} = 1 - \lambda/2 + (u_0/V_{T_e})^2/6$. We found that the trapped Langmuir waves were associated with a real frequency slightly lower than the electron plasma frequency; i.e., $\omega_r/\omega_{p_e} \approx 0.905$ for the standing hole case and $\omega_r/\omega_{p_e} \approx 0.977$ for the moving hole case with $u_0 = 0.9V_{Ti}$. These are consistent with the numerically obtained values; see Table I. For the standing hole case, the Langmuir waves are strongly Landau damped, with a damping rate $\gamma \approx 0.03\omega_{p_e}$, which is an effect not covered

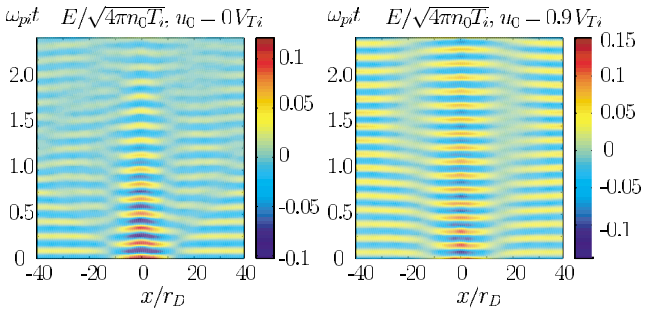

FIG. 4 (color online). Normalized Langmuir wave electric field $E/\sqrt{4\pi n_0 T_i}$ (the bipolar electric field has been removed from the data) as a function of the normalized space x/r_D and time $\omega_{p_e}t$. The Langmuir wave is trapped in the ion hole which is initially centered at $x/r_D = 0$, and moving with the speed $u_0 = 0V_{T_i}$ (left panel) and $u_0 = 0.9V_{T_i}$ (right panel).

TABLE I. Normalized frequency shifts λ and eigenfrequencies ω/ω_{p_e} for trapped small-amplitude Langmuir waves inside ion holes propagating with different speeds u_0. Theoretical values obtained from Ref. [21] (middle columns) and numerically obtained values (right columns).

Ion hole speed	Theoretical eigenfrequencies		Numerically obtained eigenfrequencies, $\omega = \omega_r - i\gamma$	
$u_0 = 0.0V_{t_i}$	$\lambda = 0.0463$	$\omega/\omega_{p_e} = 0.905$	$\omega_r/\omega_{p_e} = 0.93$	$\gamma/\omega_{p_e} = 0.03$
$u_0 = 0.9V_{t_i}$	$\lambda = 0.1906$	$\omega/\omega_{p_e} = 0.977$	$\omega_r/\omega_{p_e} = 0.98$	$\gamma/\omega_{p_e} = 0.00$

by our theoretical model [21] which is based on the electron hydrodynamic model for the Langmuir wave packets. In the moving ion hole case, the damping is significantly weaker than in the standing hole case. This can be understood in that the frequency shift is smaller for the moving ion hole case, making the scale length larger for the Langmuir wave envelope, resulting in a smaller Landau damping; some distance away from the ion hole density minimum, the potential ϕ vanishes, and there the Langmuir wave envelope decreases exponentially with ξ with the scale length $\sqrt{3/\lambda}$. A smaller λ leads to a larger length scale, resulting in a weaker Landau damping. The theoretical investigation [21] also reveals that large-amplitude trapped Langmuir waves can modify the ion hole, which then becomes wider and deeper. Physically, the broadening of the ion hole and the enhancement of negative ambipolar potential occur because the ponderomotive force of the Langmuir waves locally expels electrons, which pull ions along to maintain the local charge neutrality. The deficit of the ions in plasmas, in turn, produces more negative potential within the ion hole that is now widened and enlarged to trap the localized Langmuir wave electric field envelope.

In summary, we have used a newly developed Vlasov code to investigate the dynamics of two counterpropagating colliding ion holes, as well as the trapping of Langmuir waves in an ion hole. Our Vlasov code, which solves the Vlasov-Poisson equations in a self-consistent manner, covers the essential physics of charged particle trapping in a large-amplitude electrostatic potential, Landau damping and electron acceleration by the localized electrostatic potentials. Hence, it is capable of describing the scenario of phase space vortices and localized electric field structures which cannot be handled by means of the two fluid model [22,23]. We found that counterpropagating large-amplitude colliding ion holes are quite robust, and that during their collisions we observe the generation of nonthermal Langmuir waves on account of a two-stream instability involving accelerated electron streams that are created by the strong electrostatic potential of ion holes. Our simulation results also show that a large-amplitude ion hole can trap Langmuir waves with a frequency downshift, and is accompanied by a large bipolar electric field and a large negative potential drop in plasmas. In conclusion, we are hoping that forthcoming observations from the FAST [25] and CLUSTER [26] spacecraft missions should be able to verify the predictions of our computer simulations, which lend support to our theoretical model [21] of trapping Langmuir waves in a large-amplitude ion hole.

This research was partially supported by the SFB 591 and the EU through Contract No. HPRN-CT-2001-00314. The Swedish National Supercomputer Centre provided the computer resources for carrying out this work.

*Also at the Department of Physics, Umeå University, SE-90187 Umeå, Sweden.

[1] H. Schamel, Phys. Rep. **140**, 161 (1986); Phys. Plasmas **7**, 4831 (2000).
[2] F. Skiff *et al.*, Phys. Plasmas **8**, 3139 (2001).
[3] H. L. Berk *et al.*, Phys. Fluids **13**, 980 (1970).
[4] J. M. Grießmeier *et al.*, Phys. Plasmas **9**, 3816 (2002).
[5] H. Schamel, Plasma Phys. **13**, 491 (1971); **14**, 905 (1972).
[6] S. Bujarbarua and H. Schamel, J. Plasma Phys. **25**, 515 (1981).
[7] H. Schamel and S. Bujarbarua, Phys. Fluids **26**, 190 (1983).
[8] H. L. Pécseli *et al.*, Phys. Lett. **81A**, 386 (1981); Phys. Scr. **29**, 241 (1984).
[9] H. L. Pécseli, Laser Part. Beams **5**, 211 (1987).
[10] R. E. Ergun *et al.*, Phys. Rev. Lett. **81**, 826 (1998).
[11] R. E. Ergun *et al.*, Geophys. Res. Lett. **25**, 2041 (1998); **25**, 2025 (1998).
[12] J. Dombeck *et al.*, J. Geophys. Res. **106**, 19 013 (2001).
[13] C. Cattell *et al.*, Geophys. Res. Lett. **29**, 9 (2002).
[14] J. P. McFadden *et al.*, J. Geophys. Res. **108**, 8018 (2003).
[15] H. Matsumoto *et al.*, Geophys. Res. Lett. **30**, 1326 (2003).
[16] L. K. S. Daldorff *et al.*, Europhys. Lett. **54**, 161 (2001).
[17] S. Børve *et al.*, J. Plasma Phys. **65**, 107 (2001).
[18] H. Schamel and P. K. Shukla, Phys. Rev. Lett. **36**, 968 (1976).
[19] P. Deeskow *et al.*, Phys. Fluids **30**, 2703 (1987).
[20] H. Schamel and V. Maslov, Phys. Scr. **T82**, 122 (1999).
[21] P. K. Shukla and B. Eliasson, JETP Lett. **77**, 647 (2003).
[22] H. Schamel, J. Plasma Phys. **9**, 377 (1973).
[23] M. W. Coffey, J. Phys. A **24**, L1345 (1991).
[24] B. Eliasson, J. Sci. Comput. **16**, 1 (2001).
[25] C. W. Carlson *et al.*, Geophys. Res. Lett. **25**, 2013 (1998).
[26] See, for example, Ann. Geophys. **19**, 1195 (2001).